Boiling hysteresis of impinging circular submerged jets with highly wetting liquids

D.W. Zhou *, C.F. Ma, J. Yu

College of Environmental and Energy Engineering, Beijing Polytechnic University, Pingleyuan 100, Chaoyang District, Beijing 100022, PR China

Abstract

An experimental study was carried out to characterize the boiling hysteresis of impinging circular submerged jets with highly wetting liquids. The effects of noncondensable gases and surface aging on boiling curves were considered. The present study focused on the effects of jet parameters (jet exit velocity, radial distance from the stagnation point and nozzle diameter) and fluid subcooling on incipient boiling superheat and superheat excursion, as well as the physical mechanism of boiling hysteresis. Results show that the incipient boiling superheat decreases only with fluid subcooling regardless of jet parameters, and that the superheat excursion increases with nozzle diameter and radial distance from the stagnation point and decreasing jet exit velocity and fluid subcooling. Boiling hysteresis occurs due to deactivation of vapor embryos within larger cavities. Three anomalous phenomena at boiling inception are recorded and discussed in terms of irregular activation of vapor embryos.
© 2003 Elsevier Inc. All rights reserved.

Keywords: Jet impingement; Boiling hysteresis; Heat transfer; Highly wetting liquid

1. Introduction

Impinging jets are widely utilized where high heat transfer rates are desired, in application such as dryers, steel mills, turbine blades, electronics and microelectronics. The increased power dissipation in chips with ever-higher component densities has necessitated the search for more effective cooling techniques. In the last twenty years, progress has been made in the thermal design and control of electronic equipment driven by the utilization prospects of highly wetting liquids. However, boiling hysteresis (also termed as temperature excursion), which was observed first by Corty and Foust (1955), occurs for these liquids with unusually low surface tension and very small wetting angles on all commercial surfaces (Bar-Cohen et al., 1992). These liquids also have uncommonly high gas solubility.

Many researchers have investigated boiling hysteresis both theoretically and experimentally. As to the conditions of boiling inception, Bergles and Rohsenow (1964),

Davis and Anderson (1966), Yin and Abdelmessih (1977), Tong et al. (1990) and Shi et al. (1993) proposed analytical models based on the presence of active cavities on the heater surface. Moreover, Judd and Merte (1972), Joudi and James (1977), Bergles and Chyu (1982), Marto and Lepere (1982), Ma and Bergles (1983, 1986), Hino and Ueda (1985), Marsh and Mudawar (1989), You et al. (1990), Huang and Witte (1996) and Yu et al. (1997) reported boiling hysteresis due to variations in the size of activation cavities on the heater surface. Furthermore, Joudi and James (1977) and Yu et al. (1997) recorded temperature history traces, which are associated with wall temperature fluctuation and drop during boiling inception. The literature published prior to 1986 has been well reviewed by Bar-Cohen and Simon (1988).

A brief review on work prior to 1990 was provided by you et al. (1990) and supplemented by Yu et al. (1997) with added information on the incipient boiling superheat of highly wetting liquids. As can be seen from the collected data of Yu et al. (1997), significant variations of incipient boiling superheat are visible from one test case to another. Due to greater unsteadiness and nonrepeatability of incipient boiling superheat, these

---

* Corresponding author. Fax: +86-10-6739-2774.
E-mail address: drdwzhou@hotmail.com (D.W. Zhou).

Nomenclature

C	empirical constant
d	interior diameter of jet nozzle, m
f	nonuniformity factor of constantan foil
h	local heat transfer rate, $(q''/(T_w - T_l))$, W/(m^2 K)
h_{fg}	latent heat of vaporization, J/kg
I	current intensity, A
k	thermal conductivity, W/(m K)
m	exponent used in equation
q''	heat flux, W/m^2
q''_c	conduction heat flux, W/m^2
r	radial distance from the stagnation point, m
r/d	dimensionless radial distance from the stagnation point
r_c	radius of largest active nucleate site, m
R	electrical resistance, Ω
S	area of heated surface, m^2
t	waiting time, s
T	temperature, K

ΔT_{sat}	wall superheat, $(T_w - T_{sat})$, K
ΔT_{sub}	subcooling, $(T_{sat} - T_l)$, K
u	jet velocity, m/s
z	nozzle-to-plate spacing, m
z/d	dimensionless nozzle-to-plate spacing
Pr	Prandtl number
σ	surface tension, N/m
μ	dynamic viscosity, kg/(m s)
ρ	density, kg/m^3

Subscripts

avg	average
c	critical
l	liquid
ONB	at the onset of nucleate boiling
sat	saturation
v	vapor
w	wall

experimental data were collected only as a reference to provide a database for comparison. This impedes the fundamental understanding of the physical mechanism of boiling hysteresis.

Nucleated boiling heat transfer is noticeably affected by the surface conditions of heaters, including roughness, material, wettability (Liang and Yang, 1998), cleanliness (Joudi and James, 1981) and aging. Bergles and Chyu (1982) and Marto and Lepere (1982) performed all the tests rigorously according to well-defined procedures so as to improve the data's reproducibility. They thus obtained data with good consistency. On the other hand, You et al. (1990, 1995) proposed a statistical or probabilistic means for the presentation of experimental results. However, wide variances for their data of R113 and FC72 indicate that the advantage of this new approach should be associated with improved control of both the experimental procedure and the surface conditions. Unfortunately, few researchers in this field have adopted the experimental methods established by Bergles and Chyu or You et al.

To the knowledge of the present authors, thermal behavior at boiling inception is influenced not only by the surface condition at the moment of boiling inception but also by the thermal processes associated with the surface before this moment. The effect of the surface condition on incipient boiling superheat is more sensible for highly wetting liquids. Consequently, the experimental procedures of boiling heat transfer should be performed rigorously. Additionally, most previous tests are pertinent to pool boiling of highly wetting liquids. In this study, since L12378 (also termed PF-5052) and

R113 were used, a rigorous experimental procedure was performed. Impinging circular submerged jets were employed to determine the effects of such factors as jet parameters and fluid subcooling on incipient boiling superheat and superheat excursion. The inherent mechanism on boiling hysteresis was elucidated in light of the effective activation of vapor embryos within cavities on the heater surface. These results may lead to finding an effective way to reduce or eliminate boiling hysteresis.

2. Experimental apparatus and methods

2.1. Experimental apparatus

The overall apparatus is schematically shown in Fig. 1. R113 and L12378 were selected as the working fluids and circulated in a closed loop having provision for filtering, metering, preheating and cooling. A single flush-mounted heater was fixed vertically on one side of the chamber about 100 mm below the free surface of the pool. The main part of the test section was a strip of 10 μm thick constantan foil with a heated section of 5 mm×5 mm (nominal) exposed to the coolant. The active section of the constantan foil was used as an electrical heating element as well as a heat transfer surface since it has negligible resistance variance within a wide temperature range. The nozzles had interior diameters of 0.96 mm and 1.01 mm, and lengths of 30 mm and 35 mm. The pressure of the experiment was considered close to the atmosphere due to the flexible nature of the
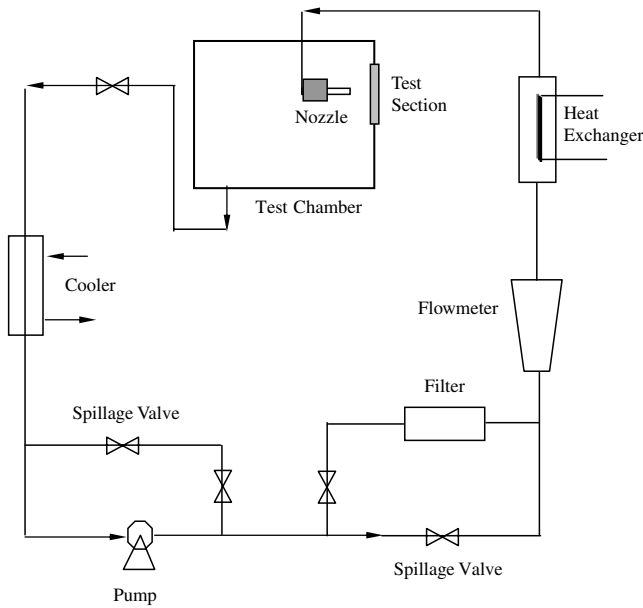
Fig. 1. Schematic layout of flow loop.

Table 1
Uncertainty analysis for heat flux

Individual measured value		$\left|\frac{\delta x_i}{q''}\frac{\partial q''}{\partial x_i}\right| \times 100$ (%)
x_i	Unit	
f	–	1.56–2.89
q''_c	W/m^2	0.41–0.94
I	A	0.27–0.56
S	m^2	0.04–0.18
R	Ω	0.03–0.16
Total uncertainty: $\delta q''/q'' = 2.64$–4.13 (%)		

The uncertainty encountered in the heat flux determination was estimated using the method suggested by Kline and McClintock (1953) with a 95% confidence level. The total uncertainty estimated for the heat flux ranged from 2.64% to 4.13%. The individual contributions to the total uncertainty are represented in Table 1. The primary contributor comes from the nonuniformity factor f of the constantan foil. Another significant source of uncertainty is the conduction heat flux q''_c and the current intensity. The uncertainties in the heat transfer rate, Reynolds number and radial position (r/d) along the heater are estimated to be within 4.32%, 1.85% and 0.65%, respectively.

3. Results and discussion

3.1. Boiling hysteresis of highly wetting liquid

The boiling curve of the conventional liquids obtained by decreasing heat flux is usually the same as that of increasing heat flux. However, the same trend does not occur for highly wetting liquids. Once boiling is initiated, the surface temperature drops sharply and then follows the typical boiling curve with increasing heat flux. If the heat flux is subsequently reduced, the surface temperature continues to follow the typical boiling curve, thereby exhibiting a hysteresis phenomenon of the boiling curve.

Fig. 2(a) and (b) represent the typical curves of boiling hysteresis for impinging circular submerged jets in the forms of q'' versus ΔT_{sat} and h versus q'', respectively. Independent of boiling type, the boiling inception was delayed to a higher wall superheat (e.g. $(\Delta T_{sat})_{ONB} = 34.51$ K for $u = 0.989$ m/s) and a higher applied heat flux in comparison with conventional boiling. Boiling curves for increasing heat flux exhibit distinct single-phase convection and nucleate boiling regimes regardless of their representation form. An area is enclosed by two curves obtained by increasing and decreasing heat flux. You et al. (1990) defined the superheat excursion at boiling inception as the maximum temperature difference (along a line of constant heat flux) between the surface temperature for increasing
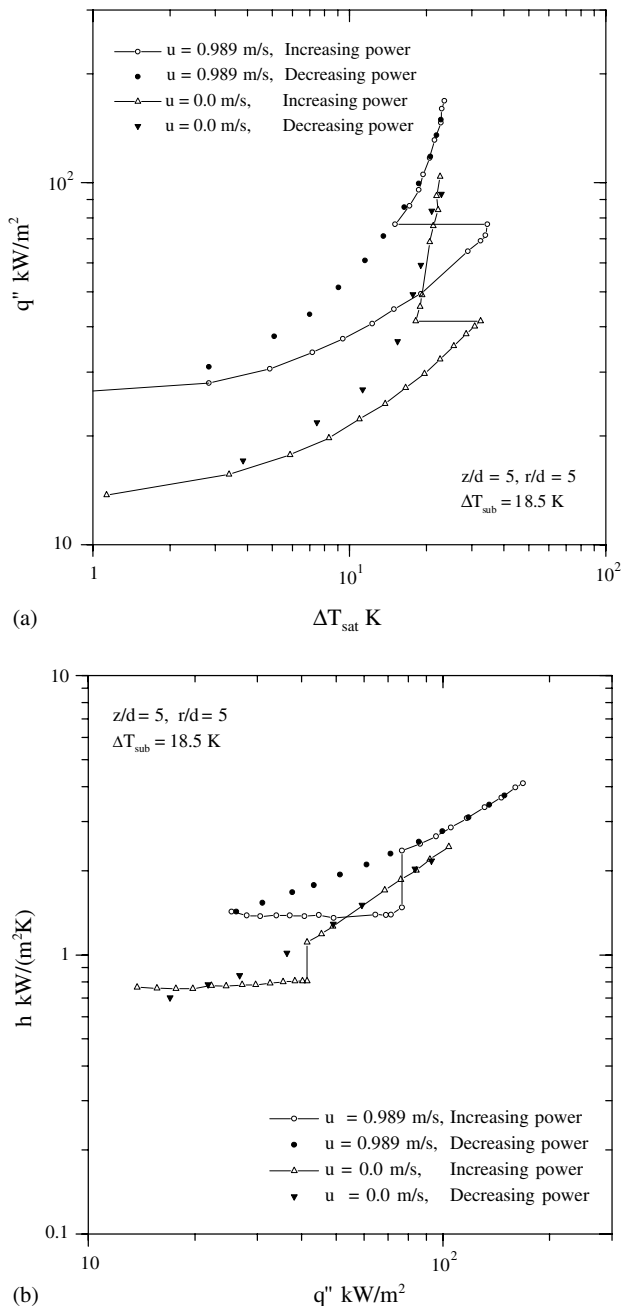
plastic seal at the top of the chamber. Further details about the experimental apparatus and rigorous procedures can be found (Zhou and Ma, 2003).

2.2. Data reduction and experimental uncertainty

The nominal heater surface heat flux was determined using the following formula:

$$q'' = fI^2R/S, \qquad (1)$$

where the nonuniformity factor of the constantan foil, $f \approx 1$, was adopted for the heat flux calculation and yet it contributed largely to the uncertainty in total heat flux evaluation. The resistance R was measured accurately with direct current before the experiment. The area S of the heater surface was measured for each test section with a tool-maker's microscope of 1 μm resolution.

The temperature of the jet fluid was controlled with an auxiliary heater situated before the nozzle exit so that the temperature difference between the jet fluid and the bulk fluid was less than ±0.5 K. The local heat transfer rate was calculated from the heat flux, the wall temperature T_w and the bulk fluid temperature T_l as follows:

$$h = (q'' - q''_c)/(T_w - T_l). \qquad (2)$$

Heat flux to the back of the heater q''_c was estimated by heat conduction analysis. With jet impingement, the conduction loss is less than 1% of power input to the heater. Heat loss through the bakelite was estimated as only 0.1% of the power input. Unless otherwise indicated, the tests were performed according to a rigorous procedure, and the data are for R113 and nozzle-to-plate spacing of $z/d = 5$.

Fig. 2. Typical boiling curves of highly wetting liquid: (a) q'' versus ΔT_{sat} and (b) h versus q''.

heat flux and that for decreasing heat flux. For pool and impingement boiling, the superheat excursions are 8.38 and 19.42 K, where the heat transfer rates shown in Fig. 2(b) increase drastically from 0.80×10^3 and 1.48×10^3 to 1.11×10^3 and 2.36×10^3 W/(m^2 K), respectively.

The boiling was initiated at the so-called nucleation cavities, which harbor residual vapor or noncondensable gas. If a vapor embryo is released from a cavity, the surrounding liquid enters the cavity and the shape of the advancing liquid front is determined by its wetting angle. For conventional liquids or rough heated surfaces,

the wetting angle exceeds the effective cone angle of the cavity and the liquid cannot fill the cavity; thereby, residual vapor is trapped and held for a nucleation site. The boiling occurs at lower wall superheat and applied heat flux.

Hsu (1962) confirmed that the activation of nucleation nuclei within greater cavities on the smooth surface was only possible for larger superheats or in the presence of a relatively thick superheated liquid boundary layer. As highly wetting liquids were used, they flooded all but the smallest cavities, depleting vapor embryos needed for the boiling inception (Bar-Cohen and Simon, 1988). The heater surface dissipates the heat only by conduction and convection before the vapor embryo is activated to boiling. Extensive deactivation of nucleation sites by flooding would then require elevated wall temperatures to initiate bubbles at the remaining smaller cavities. The wall superheat increases with applied heat flux until the cavities, which are below the size flooded by the working fluid, can trap residual vapor. Shoukri and Judd (1975) verified that smaller cavities were better able to entrap vapor residues and were activated more easily by their neighbor when boiling was initiated. This implies that higher incipient boiling superheat demand corresponds to smaller cavities available to initiate boiling. In this limited case, homogeneous nucleation in the bulk liquid would take place. Once vapor embryos obtain enough energy to nucleate and then separate from the cavities, boiling takes place. Therefore, boiling hysteresis is a macro-manifestation of the vapor embryos' deactivation on the heater surface. This occurs due to the smooth heater surface, and is exacerbated by the small surface tension of the working fluids. Based on the analysis above, boiling hysteresis is accompanied with lower heat transfer rates prior to boiling inception.

Since highly wetting liquids typically can absorb large amounts of noncondensable gases, a thorough examination of dissolved gases effect on boiling behaviors is needed. Fig. 3 shows the effect of noncondensable gas on L12378 pool boiling. Boiling curves without degassing have poor repeatability, especially in the vicinity of boiling inception. Comparison with boiling curves of degassing indicated that the dissolved gases enhanced heat transfer everywhere, leading to lower incipient boiling superheat. This is primarily attributed to the fact that the dissolved gases decrease the saturation temperature in nature and thus decrease the surface tension of highly wetting liquids (Bar-Cohen et al., 1992) on one hand and bring nucleation embryos to boiling on the other hand. The effect of noncondensable gas on heat transfer decreases at higher heat flux.

Surface aging is another important factor influencing boiling behaviors of highly wetting liquids. Joudi and James (1981) considered that surface aging was reflected in the inconsistency and scatter of experimental data
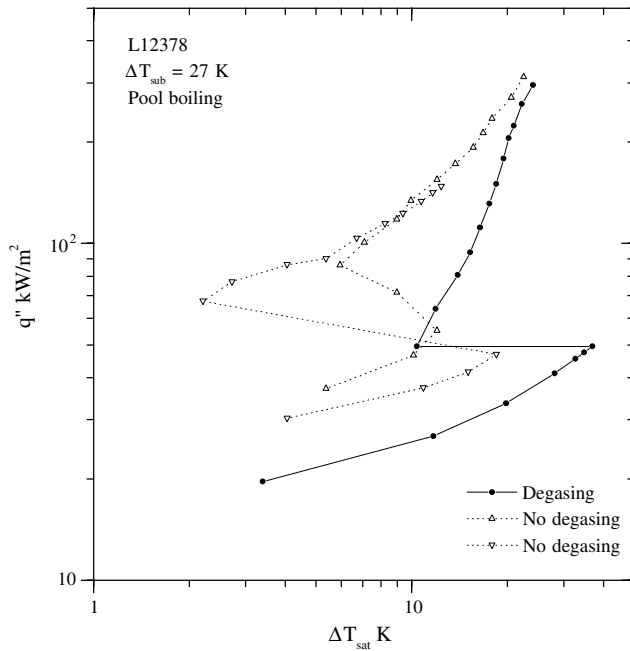
Fig. 3. Effect of noncondensable gas on the boiling curve.

caused by the "time-in-use" or so-called aging of a surface on which boiling occurs. Fig. 4 depicts the surface aging effect on boiling curves. All the data were taken from the same test section and the working fluid was fully degassed. As the immersion time of the heater surface was increased from 1 to 10 h, the whole boiling curve shifted to the left, causing lower incipient boiling superheat. More test results showed that the boiling heat
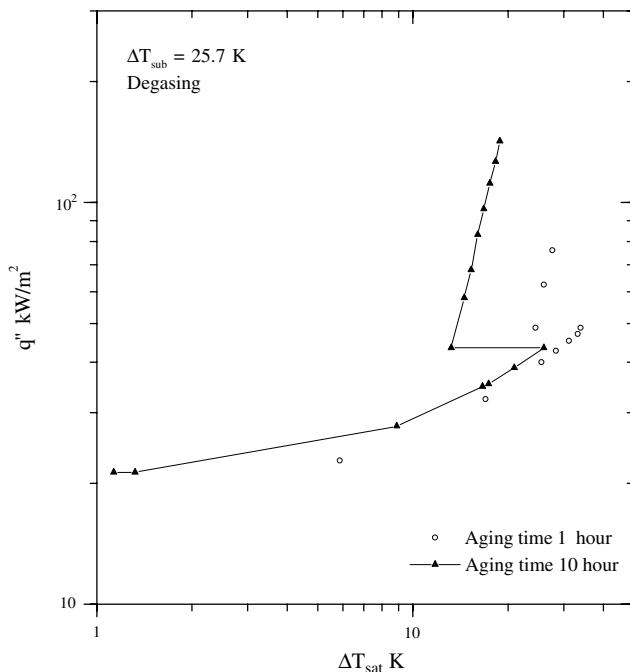

Fig. 4. Effect of surface aging of the heater on the boiling curve.

transfer was enhanced owing to the surface aging and that, as the constantan foil was submerged in the pool of L12378 and R113 at room temperature for about ten hours, the experimental data have good reproducibility.

3.2. Incipient boiling superheat and superheat excursion

Experiments were performed in detail to study the effects of jet parameters and fluid subcooling on incipient boiling superheat and superheat excursion. The results are represented in Fig. 5. Seven boiling curves obtained with the same test section at $\Delta T_{sub} = 18.5$ K and $r/d = 2$ were plotted in Fig. 5(a) to determine the effect of jet exit velocity on boiling hysteresis. In this study, the pool boiling represented the limiting case of zero velocity. The boiling occurs approximately at $(\Delta T_{sat})_{ONB} = 34$ K for pool and impingement boiling except for a case of $u = 1.062$ m/s. The superheat excursion decreases with jet exit velocity due to heat transfer enhancement of impinging jets and disappears as the jet exit velocity exceeds 10 m/s. An excess value of incipient boiling superheat between 1–3 K was observed by Yin and Abdelmessih (1977) for an R11 flow boiling in a stainless steel tube, and was considered to be independent of the flow velocity in the tested range. Hino and Ueda (1985) and Marsh and Mudawar (1989) reported similar results. Referring to the data of Ma and Bergles (1983) and Bar-Cohen and Simon (1988) indicated that for both pool and impingement boiling the nucleation appeared to occur at the same wall superheat.

The test section must return to the initial state after a run so as to ensure identical initial test conditions for all the data. This takes the test section a certain delay time between runs. Table 2 lists the delay time for every run. Compared with the other runs, the delay time of only 40 min for $u = 1.062$ m/s was so short that the test section did not have enough time to cool down. R113s insufficient wetting on the heater surface before the test resulted in noncondensable gas harboring within some larger cavities, where it contributes to a lower incipient boiling superheat.

Few previous works examined the effect of radial distance from the stagnation point on boiling hysteresis. For R113 submerged jets, Ma and Bergles (1983) only presented their experimental data of boiling hysteresis but did not give an explanation for the relation between them. Variations of incipient boiling superheat and superheat excursion with radial distance from the stagnation point are shown in Fig. 5(b) and (c). Independent of jet exit velocity and nozzle diameter, the present study and Ma and Bergles' (1983) data show that the radial distance from the stagnation point has a negligible influence on incipient boiling superheat. With decreasing radial distance from the stagnation point, the boiling curves extend to higher wall superheat at higher heat
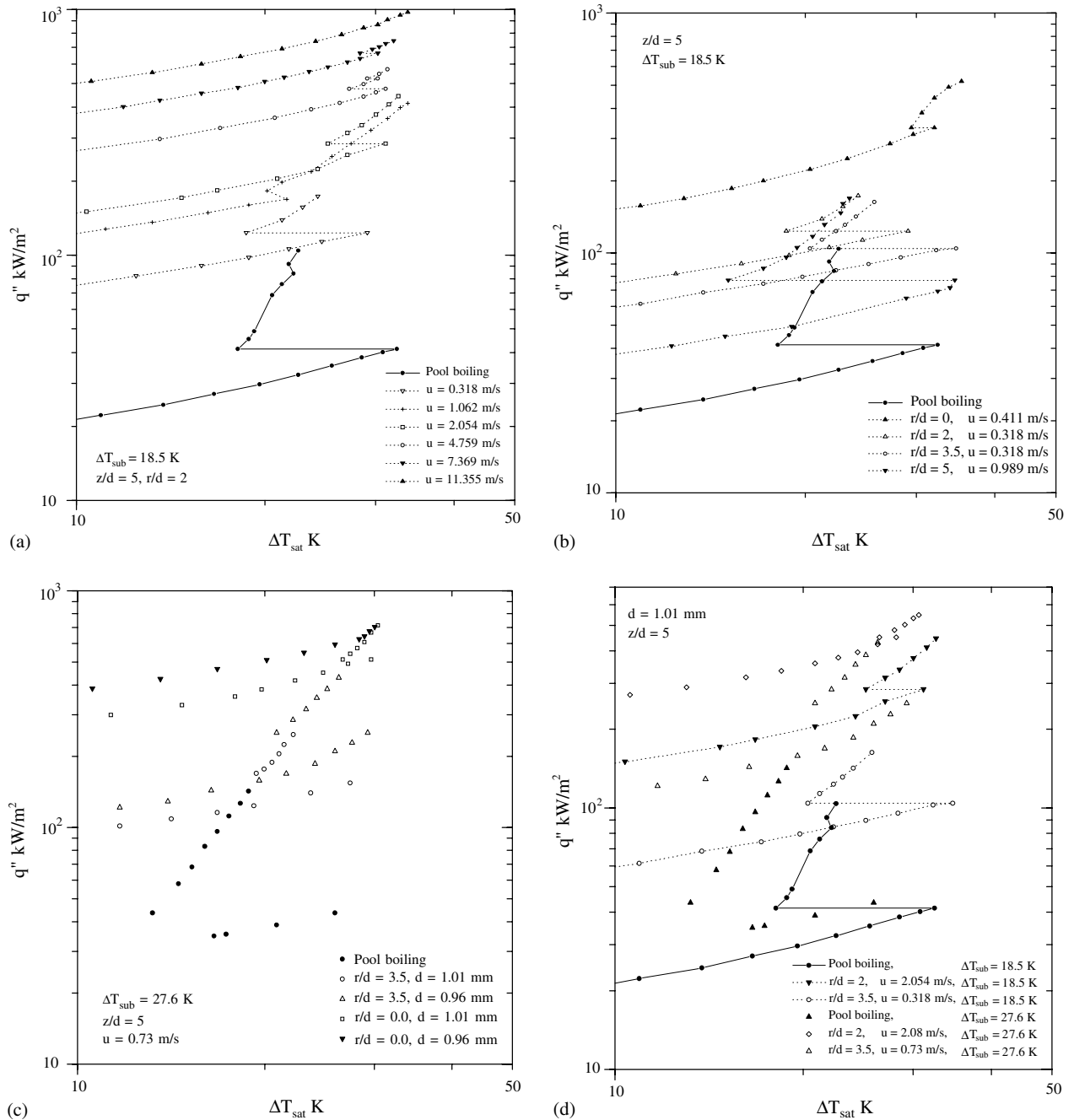
Fig. 5. (a–d) Effects of jet parameters and fluid subcooling on incipient boiling superheat and superheat excursion.

flux, leading to lower superheat excursion. The effect of the nozzle diameter on boiling hysteresis is also represented in Fig. 5(c). The nozzle diameter causes a quite weak difference in incipient boiling superheat (e.g. 1.86 K for $r/d = 3.5$). Considering the complexity of nucleate boiling heat transfer, this degree of discrepancy is acceptable. The superheat excursion increases with nozzle diameter.

The effect of fluid subcooling on incipient boiling superheat and superheat excursion is shown in Fig. 5(d). For $\Delta T_{sub} = 18.5$ K, boiling inception occurs at about 32

K regardless of jet exit velocity and radial distance from the stagnation point. As the fluid subcooling is increased to 27.6 K, the incipient boiling superheat decreases to 27 K due to an increase of surface tension resulting in an increased capability to trap residual vapor. Fluid subcooling effect on incipient boiling superheat is in agreement with Ma and Bergles' (1986) results for submerged jets and Yu et al. (1997) results for pool boiling. The superheat excursion decreases at higher fluid subcooling.

Based on the above-mentioned analysis, the incipient boiling superheat is related only to fluid subcooling

Table 2
The delay time between runs

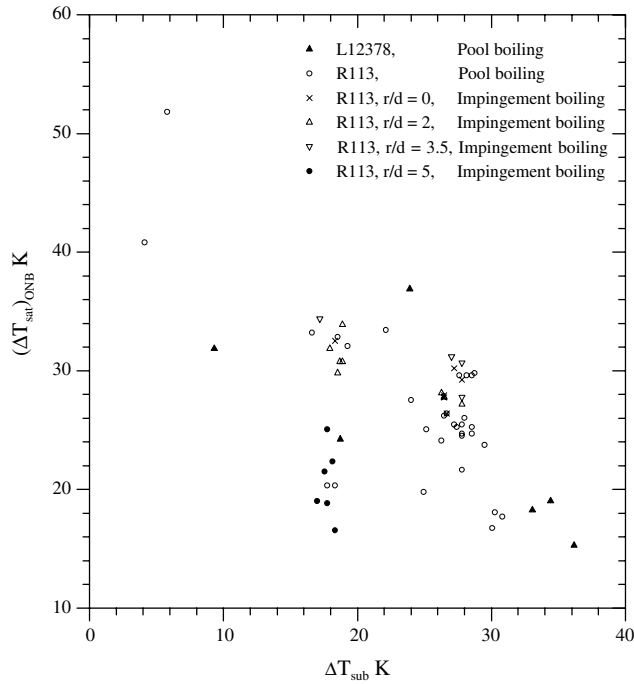| Jet exit velocity u (m/s)	0	0.318	1.062	2.054	4.759	7.369	11.355
Delay time t (min)	80	60	40	80	60	60	55

Fig. 6. Variation of incipient boiling superheat with fluid subcooling and radial distance from the stagnation point.

irrespective of jet parameters. In order to illustrate further the fluid subcooling effect, all the incipient boiling superheat data were collected and represented in Fig. 6. The incipient boiling superheat decreases with fluid subcooling. The prediction of the incipient boiling superheat was represented as

$$(\Delta T_{sat})_{ONB} = C(\Delta T_{sub})^m. \tag{3}$$

The correlated results are listed in Table 3 within $\pm 10\%$. Coefficient C and the exponent m of Eq. (3) remain almost unchanged for R113 with the exception of $r/d = 5$. This was believed to be the result of fewer experimental data obtained for this case. Comparisons of pool boiling data between R113 and L12378 indicate

that there is a weak discrepancy between them due to similar saturation temperatures. Table 4 listed the thermophysical properties of L12378 and R113.

Next, the relation between heat flux and the incipient boiling superheat is considered. As proposed by Bergles and Rohsenow (1964), boiling inception is defined as the first significant increase of the heat transfer rate from that predicted for single phase forced convection. However, when reducing the heat flux, boiling persists until a lower wall superheat is reached. This lower incipient boiling superheat is different from the former and characterizes the boiling surface because it represents stable and established boiling behavior (Ma and Bergles, 1986; Hino and Ueda, 1985). Bergles and Rohsenow (1964) and Davis and Anderson (1966) proposed the following correlations for the termination point of nucleate boiling. In the case where the surface cavities of all sizes are available for nucleation:

$$q'' = (T_w - T_{sat}) \frac{h_{fg} k_1 \rho_v}{8 T_{avg} \sigma}. \tag{4}$$

In the case where the upper limit of nucleation cavity sizes is restricted to radius r_c, the incipient boiling condition is expressed as follows:

$$q'' = \frac{k_1 (T_w - T_{sat})}{r_c} - \frac{2\sigma k_1 T_{avg}}{h_{fg} \rho_v r_c^2}, \tag{5}$$

where $T_{avg} = (T_w + T_{sat})/2$, and h_{fg}, ρ_G and σ are the latent heat of evaporation, vapor density and surface tension, respectively.

Comparisons of lower incipient boiling superheat between the present data and the predicted values of Eqs. (4) and (5) are depicted in Fig. 7. The present heat flux at the termination point of nucleate boiling has the same order as that for R113 impingement boiling given by Ma and Bergles (1986) and is about one order higher than that for flow boiling given by Hino and Ueda (1985). The present data shown in Fig. 7 are less than those predicted from Eq. (4) and yet bounded by Eq. (5), demonstrating

Table 3
Correlated results of incipient boiling superheat

Working fluid	Boiling type	r/d	C	m	Range of ΔT_{sub}/K
L12378	Pool	–	116.11	−0.151	9–37
R113	Pool	–	116.04	−0.1436	4–31
R113	Impingement	0	116.36	−0.1302	18–27
R113	Impingement	2	115.55	−0.1308	17–28
R113	Impingement	3.5	116.27	−0.1232	16–27
R113	Impingement	5	103.98	−0.1479	15–20
R113	Pool/Impingement	–	116.34	−0.1358	4–31

Table 4
The thermophysical properties of L12378 and R113 at standard state

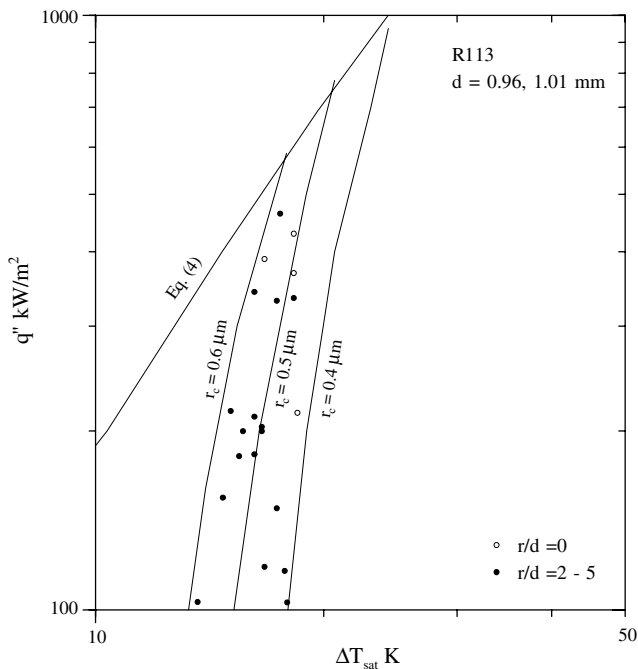| Working fluid	T_{sat}/K	ρ_l/kg/m³	μ/kg/(m s)	σ/N/m	h_{fg}/J/kg	Pr
L12378	323	1700	6.8E−4	1.3E−2	1.045E+5	11.7
R113	321	1511	5.03E−4	1.47E−2	1.47E+5	7.01

Fig. 7. Comparison of the termination point of nucleate boiling between the experimental and predicted values.

the limited size of nucleation cavities. Since the present constantan foil was taken from the same manufacturing run as that of Ma and Bergles (1983, 1986), the cavity size corresponding to the termination point of nucleate boiling, which can be activated to initiate the boiling, varies in the range of r_c = 0.4–0.6 μm, too. As shown in Fig. 2, the incipient boiling superheat for heat flux increase is markedly higher than the termination point of nucleate boiling. The cavity size for the former is therefore less than the value of 0.4–0.6 μm. The optical observation by Ma and Bergles (1986) with a scanning electron microscope showed that the pits and depressions on the surface of the constantan foil were in the range of 0.2–1.2 μm. It was concluded that it is within cavities on the heater surface that vapor embryos activate, grow up and separate. Since the effects of jet parameters in this study cannot reach the interior surface of these cavities, the incipient boiling superheat is irrelevant to jet parameters.

3.3. Anomalous phenomena at boiling inception

Three anomalous phenomena at boiling inception occur infrequently for immersion cooling of the smooth surface with highly wetting liquids. Although the power to the test section was reduced, as shown in Fig. 8 for ΔT_{sub} = 26 K, the wall superheat increased abruptly from 14.85 to 19.59 K due to deactivation of the few remaining nucleation sites, resulting in the sudden termination of boiling heat transfer. Park and Bergles (1988) reported this phenomenon using the same kind of test section.

The superheat excursion is characterized by larger temperature reduction over the entire heater surface. On other occasions, a relatively small temperature decrease (6 K) took place at boiling inception at low applied heat flux, as shown in Fig. 9. Then another temperature decrease (6 K) occurred after an increase in heat flux. Thereafter, fully developed nucleate boiling became established. The occasional two-step overshoot is attributed to an irregular distribution of bubble nucleation sites near the location of the thermocouple junction. The first overshoot is believed to be the result of a few boiling sites below the location of the thermocouple. Upstream bubbles brush the top surface of the heater and enhance its heat transfer rates, suppressing the boiling inception there. The second overshoot occurs when the nucleation sites beyond the location of the thermocouple finally become active (Park and Bergles, 1988).
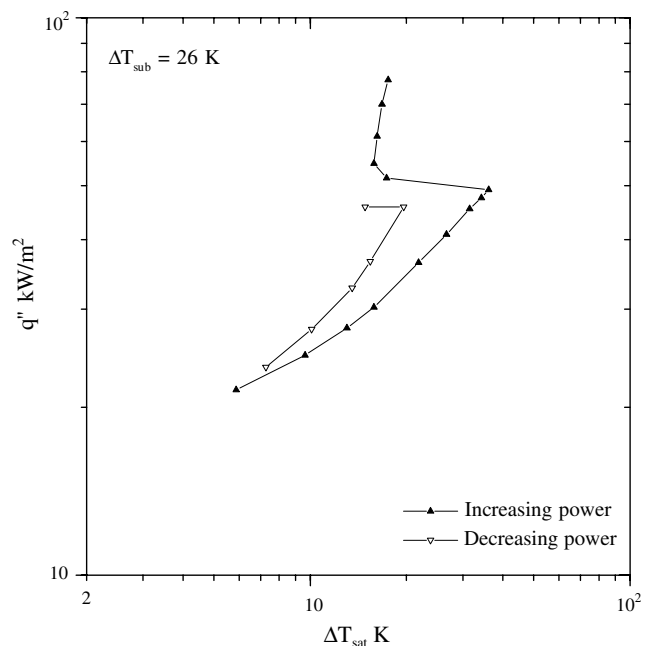

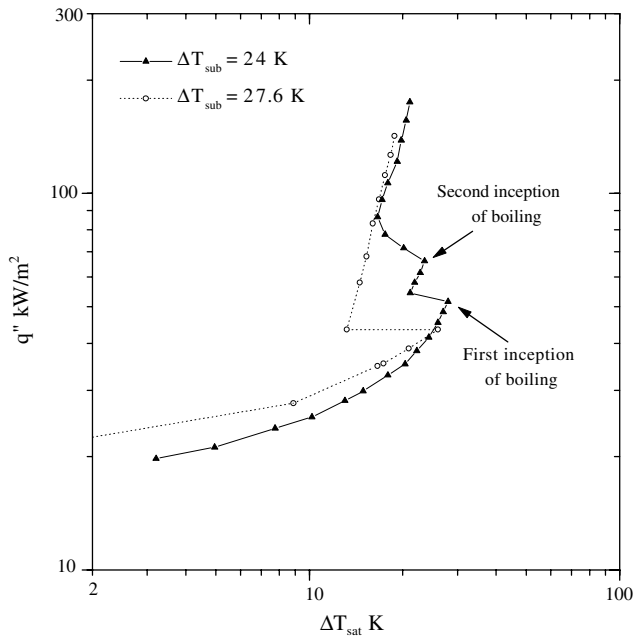Fig. 8. Wall temperature increase with decreasing heat flux.

Fig. 9. Two-step overshoot at the boiling inception.

The boiling inception of highly wetting liquids is delayed to a higher wall superheat, which is far above the saturation temperature of the working fluid. As shown in Fig. 10, boiling with superheat excursion of 25.74 and 23 K occurred at $(\Delta T_{\text{sat}})_{\text{ONB}} = 52.1$ and 47.6 K for $\Delta T_{\text{sub}} = 4.7$ and 28.4 K, respectively. The boiling curve obtained by decreasing heat flux had the same trend as the typical boiling curve regardless of fluid subcooling. This phenomenon happened when the heater surface was submerged into the working fluid at subcooled
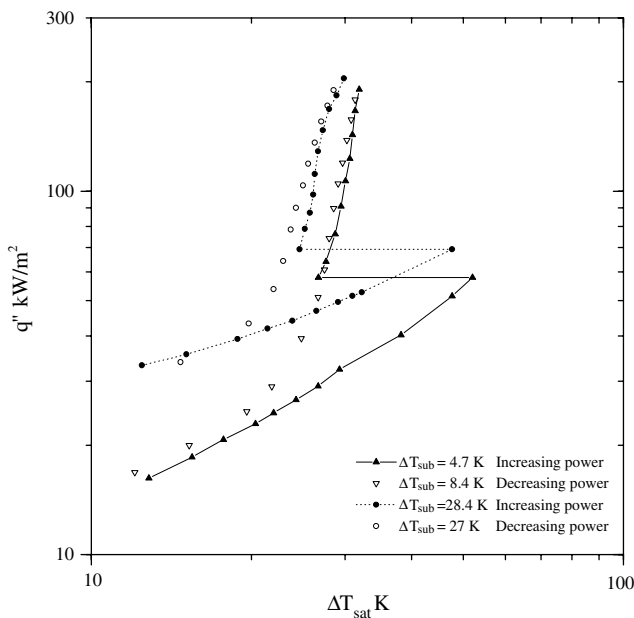

Fig. 10. Boiling curves with significantly higher incipient boiling superheat.

temperatures for periods of 20–30 min between tests. So high incipient boiling superheat has been reported only by Joudi and James (1977) (53 K) from a horizontal stainless steel flat surface with R113, by You et al. (1990) (53 K) from a thin Pt film heater with R113, and by Chang and You (1998) (52 K) using a flat, smooth surface with FC-72 and FC-87. This is believed to be related to the surface roughness, the temperature history of the bulk fluid and the heating procedure prior to boiling inception. It may represent a limiting case of heterogeneous nucleation, and it increases the risk of transitioning directly to film boiling from single-phase convection. This is because direct transition from single-phase convection to film boiling can be observed at the incipient boiling superheat when the heat flux at boiling inception is higher than the minimum heat flux of the boiling curve and the incipient boiling superheat is higher than the transition boiling curve value at the incipient heat flux (Chang and You, 1998). Once boiling occurs, film boiling actually covers a portion of the surface momentarily. Thereby, it appears that the nucleate boiling regime is bypassed and the mode of heat transfer is film boiling over the heat transfer area due to a great temperature difference. However, since the applied heat flux (about $5–7 \times 10^4$ W/m^2) is not high enough to sustain this boiling mode, the surface temperature drops and then steady nucleate boiling becomes established.

For the significantly higher incipient boiling superheat, whether the boiling occurs or not through homogeneous nucleation in the bulk liquid. Based on the homogeneous nucleation model, Bar-Cohen and Simon (1988) obtained an upper boundary for the incipient boiling superheat and it is of the form:

$$(\Delta T_{\text{sat}})_{\text{ONB}} \leqslant T_c \left[0.923 - \frac{T_{\text{sat}}}{T_c} + 0.077 \left(\frac{T_{\text{sat}}}{T_c} \right)^9 \right]. \qquad (6)$$

For the case of R113 with a critical temperature of 487 K, it is interesting to note that Eq. (6) yields an incipient boiling superheat in excess of $(\Delta T_{\text{sat}})_{\text{ONB}} = 102$ K in the standard state. Comparison of incipient boiling superheat between the predicted value of Eq. (6) and the present datum (52.1 K) indicates that boiling is initiated through heterogeneous nucleation rather than homogeneous nucleation.

4. Conclusions

The most important findings of this study are:

(1) Boiling hysteresis occurs with a lower heat transfer rate prior to boiling inception. Both noncondensable gases and surface aging can enhance heat transfer.
(2) Incipient boiling superheat decreases only with fluid subcooling regardless of jet parameters. Superheat excursion increases with nozzle diameter and radial

distance from the stagnation point and with decreasing jet exit velocity and fluid subcooling.

(3) For highly wetting liquids, it is from the interior surface within cavities on the smooth heater surface that vapor embryos activate, grow up and separate. Higher incipient boiling superheat demand corresponds to smaller cavities that are available to initiate boiling.

(4) Boiling hysteresis results from the deactivation of vapor embryos within larger cavities while three anomalous phenomena at boiling inception observed in this study are closely associated with irregular nucleation.

Acknowledgements

References

Bar-Cohen, A., Simon, T.W., 1988. Wall superheat excursions in the boiling incipience of dielectric fluids. Heat Transfer Eng. 9 (3), 19–31.

Bar-Cohen, A., Tong, W., Simon, T.W., 1992. Theoretical aspects of nucleate pool boiling with dielectric liquids. J. Therm. Sci. 1 (1), 46–51.

Bergles, A.E., Chyu, M.C., 1982. Characteristics of nucleate pool boiling from porous metallic coatings. J. Heat Transfer 104 (5), 279–285.

Bergles, A.E., Rohsenow, W.M., 1964. The determination of forced convection surface boiling heat transfer. J. Heat Transfer 86 (8), 365–370.

Chang, J.Y., You, S.M., 1998. Film boiling incipience at the departure from natural convection on flat, smooth surfaces. J. Heat Transfer 120 (5), 402–409.

Corty, C., Foust, A.S., 1955. Surface variables in nucleate boiling. Chem. Eng. Prog. Symp. Ser. 51 (17), 1–12.

Davis, E.J., Anderson, G.H., 1966. The incipience of nucleate boiling in forced convection flow. AIChE J. 8 (7), 774–779.

Hino, R., Ueda, T., 1985. Study on heat transfer and flow characteristics in subcooled flow boiling. Part 1: boiling characteristics. Int. J. Multiphase Flow 11 (3), 269–281.

Hsu, Y.Y., 1962. On the size range of active nucleation cavities on a heating surface. J. Heat transfer 34 (8), 207–214.

Huang, L., Witte, L.C., 1996. An experimental investigation of the effects of subcooling and velocity on boiling of freon-113. J. Heat Transfer 118 (5), 436–442.

Joudi, K.A., James, D.D., 1977. Incipient boiling characteristics at atmospheric and subatmospheric pressures. J. Heat Transfer 99 (8), 398–403.

Joudi, K.A., James, D.D., 1981. Surface contamination, rejuvenation, and the reproducibility of results in nucleate pool boiling. J. Heat Transfer 103 (8), 453–460.

Judd, R.L., Merte, H., 1972. Evaluation of nucleate boiling heat flux predictions at varying levels of subcooling and acceleration. Int. J. Heat Mass Transfer 15 (6), 1075–1096.

Kline, S.J., McClintock, F.A., 1953. Describing uncertainties in single-sample experiments. Mech. Eng. 75, 3–8.

Liang, H.S., Yang, W.J., 1998. Nucleate pool boiling heat transfer in a highly wetting liquid on micro-graphite fiber composite surfaces. Int. J. Heat Mass Transfer 41 (13), 1993–2000.

Ma, C.F., Bergles, A.E., 1983. Boiling jet impingement cooling of simulated microelectronic chips. In: Oktay, S., Bar-Cohen, A. (Eds.), Heat Transfer in Electronic Equipment, vol. 28. ASME, New York, pp. 5–12.

Ma, C.F., Bergles, A.E., 1986. Jet impingement nucleate boiling. Int. J. Heat Mass Transfer 29 (2), 1095–1100.

Marsh, W.J., Mudawar, I., 1989. Sensible heating and boiling incipience in free-falling dielectric liquid films. J. Electron. Packaging 111 (3), 46–51.

Marto, P.J., Lepere, V.J., 1982. Pooling boiling heat transfer from enhanced surfaces to dielectric fluids. J. Heat Transfer 104 (5), 292–298.

Park, K.A., Bergles, A.E., 1988. Effects of size of simulated microelectronic chips on boiling and critical heat flux. J. Heat Transfer 110 (8), 728–732.

Shi, M.H., Ma, J., Wang, B.X., 1993. Analysis on hysteresis in nucleate pool boiling heat transfer. Int. J. Heat Mass Transfer 36 (18), 4461–4466.

Shoukri, M., Judd, R.L., 1975. Nucleation site activation in saturated boiling. J. Heat Transfer 97 (2), 93–96.

Tong, W., Bar-Cohen, A., Simon, T.W., 1990. Contact angle effects on boiling incipience of highly-wetting liquids. Int. J. Heat Mass Transfer 33 (1), 91–100.

Yin, S.T., Abdelmessih, A.H., 1977. Prediction of incipient flow boiling from a uniformly heated surface. Nucl. Sol. Process Heat Transfer-St. Louis 73, 236–242.

You, S.M., Simon, T.W., Bar-Cohen, A., Tong, W., 1990. Experimental investigation of nucleate boiling incipience with a highly wetting dielectric fluid (R113). Int. J. Heat Mass Transfer 33, 105–117.

You, S.M., Simon, T.W., Bar-Cohen, A., Hong, Y.S., 1995. Effects of dissolved gas content on pool boiling of a highly-wetting fluid. J. Heat Transfer 117, 687–692.

Yu, J., Ma, C.F., Tien, S.R., Honda, H., 1997. Effects of surface condition and fluid subcooling on incipient and developed nucleate boiling of highly-wetting liquids. Chin. J. Eng. Thermophys. 17 (3), 47–50.

Zhou, D.W., Ma, C.F., 2003. Local jet impingement boiling heat transfer with R113. Heat Mass Transfer 40 (2), 88–99.